The Australian Journal of Mathematical Analysis and Applications

AJMAA

Volume 10, Issue 1, Article 14, pp. 1-17, 2013

NUMERICAL SOLUTION OF A SYSTEM OF SINGULARLY PERTURBED CONVECTION-DIFFUSION BOUNDARY-VALUE PROBLEMS USING MESH EQUIDISTRIBUTION TECHNIQUE

PRATIBHAMOY DAS AND SRINIVASAN NATESAN

Received 2nd May, 2013; accepted 21 June, 2013; published 4 November, 2013.

DEPARTMENT OF MATHEMATICS, INDIAN INSTITUTE OF TECHNOLOGY GUWAHATI, GUWAHATI - 781 039, INDIA.
pratibhamoy@gmail.com
natesan@iitg.ernet.in
URL: http://www.iitg.ernet.in/natesan/

ABSTRACT. In this article, we consider a system of singularly perturbed weakly coupled convection-diffusion equations having diffusion parameters of different magnitudes. These small parameters give rise to boundary layers. An upwind finite difference scheme on adaptively generated mesh is used to obtain a suitable monitor function that gives first-order convergence which is robust with respect to the diffusion parameters. We present the results of numerical experiments for linear and semilinear system of differential equations to support the effectiveness of our preferred monitor function obtained from theoretical analysis.

Key words and phrases: System of singularly perturbed convection-diffusion problems, Upwind scheme, Adaptive mesh, Uniform convergence.

2000 *Mathematics Subject Classification.* AMS 65L10.

ISSN (electronic): 1449-5910

© 2013 Austral Internet Publishing. All rights reserved.

1. INTRODUCTION

Solutions of singular perturbation problems (SPPs) exhibit sharp boundary or/and interior layers in narrow regions where solution has steep gradient. Typical applications of SPPs are boundary layers appearing in viscous fluid flow and concentration or thermal layers in mass and heat transfer. Because of the presence of the perturbation parameter, standard numerical methods on uniform meshes fail to give accurate approximation. Unless a sufficiently large number of mesh points are used inside the layer, the layers are not been resolved and the rate of convergence is far less than the non singularly perturbed problems. This phenomenon leads to develop the concept of ε-uniform numerical methods; in which the order of convergence and the error constant are independent of the singular perturbation parameter ε.

If the location and width of the layer are known *apriori*, one can invoke this knowledge to construct a suitable *apriori* layer adapted mesh. Several work are done by using *apriori* chosen meshes (*for e.g.,* well known piecewise-uniform Shishkin mesh, Bakhvalov mesh) to get uniform convergence (see [12]). Recently there is much interest in the generation of layer adapted meshes using the computed numerical solution, where solution adaptive algorithm attempts to automatically detect the location, height and thickness of the boundary layer. This paper is concerned to generate layer adapted mesh for system of weakly coupled (coupled through the reaction terms) convection-diffusion problems.

In recent years, *apriori* grid generation for system of boundary-value problems have attracted several authors. A variety of uniformly convergent numerical methods on reaction-diffusion as well as for convection-diffusion system of equations is developed. For the weakly coupled convection-diffusion system of equations, Bellew and O'Riordan [4], Linß [10] and Zhongdi [13] carried out the analysis on *apriori* chosen Shishkin and Bakhvalov meshes. Singularly perturbed system of reaction-diffusion problems are considered by Das and Natesan [7] where a hybrid scheme is proposed on Shishkin type meshes.

In this article, we consider the following system of weakly coupled singularly perturbed convection-diffusion boundary-value problem (BVP):

$$\begin{cases} \mathbf{L}\boldsymbol{u} \equiv -\boldsymbol{Eps}\,\boldsymbol{u}''(x) - \boldsymbol{A}(x)\boldsymbol{u}'(x) + \boldsymbol{B}(x)\boldsymbol{u}(x) = \boldsymbol{f}(x), \; x \in \Omega = (0,1), \\ \boldsymbol{u}(0) = \boldsymbol{u}(1) = \mathbf{0}, \end{cases} \tag{1.1}$$

where $\mathbf{L} = (\mathbf{L}_1, \cdots, \mathbf{L}_k)^T$, $\boldsymbol{Eps} = \mathrm{diag}(\varepsilon_1, \varepsilon_2, \cdots, \varepsilon_k)$, $\boldsymbol{A}(x) = \mathrm{diag}(a_{11}(x), a_{22}(x), \cdots, a_{kk}(x))$, $\boldsymbol{B}(x) = (b_{ij}(x))_{k\times k}$, $\boldsymbol{f}(x) = (f_1(x), f_2(x), \cdots, f_k(x))^T$ and $\boldsymbol{u}(x) = (u_1(x), \cdots, u_k(x))^T$.

Without loss of generality, we shall assume that $\min\big\{a_{11}(x), a_{22}(x), \cdots, a_{kk}(x)\big\} \geq \alpha > 0$, for $x \in \overline{\Omega} = [0,1]$. The analysis provided here, can be extended for a more general class of system of BVPs, where all $a_{ii}(x)$ are bounded away from zero by a positive constant. We shall consider the matrix $\boldsymbol{B} = (b_{ij})_{i,j=1}^{k}$, as a L_0-matrix (*i.e.,* off-diagonals are nonpositive and diagonals are positive) with

$$\min_{x\in[0,1];m=1:k} \left\{ \sum_{j=1}^{k} b_{mj}(x) \right\} \geq \beta > 0. \tag{1.2}$$

It will be assumed that the entries of the coefficient matrices ***A, B, f***, *i.e.,* a_{ii}, b_{ij}, f_i are in $\mathcal{C}^2(\overline{\Omega})$ for $i, j = 1, \cdots, k$.

A commonly used technique in adaptive grid generation is based on the idea of equidistribution. A grid $\Omega^N \equiv \{0 = x_0 < x_1 < \cdots < x_N = 1\}$ is said to be equidistributed, if

$$\int_{x_{i-1}}^{x_i} M\big(s, \boldsymbol{u}(s)\big)ds = \int_{x_i}^{x_{i+1}} M\big(s, \boldsymbol{u}(s)\big)ds, \quad i = 1, \ldots, N-1, \tag{1.3}$$

where $M\big(x,\boldsymbol{u}(x)\big)(>0)$ is called the monitor function. Equivalently, (1.3) can be expressed as

$$\int_{x_{i-1}}^{x_i} M\big(s,\boldsymbol{u}(s)\big)ds = \frac{1}{N}\int_0^1 M\big(s,\boldsymbol{u}(s)\big)ds, \quad i=1,\ldots,N. \tag{1.4}$$

It is common to use monitor functions which are bounded away from zero to maintain an appropriate distribution of mesh points throughout the domain. In practice, the monitor function is often based on simple functions, involving the derivatives of the unknown solution. In this context, Beckett and Mackenzie proposed a curvature–type monitor function for both convection-diffusion [2] as well as reaction-diffusion [3] type problem for a scalar BVP. These monitor function are based on the singular component of the solution.

This article is devoted for a system of weakly coupled convection-diffusion BVPs by generalizing the monitor function proposed by Beckett and Mackenzies [2, 3]. It should be noted that in [2], Beckett and Mackenzie carried out the convergence analysis by assuming the convection term as a constant, and the grid is obtained by using the equidistribution of the exact solution. For our case, we have carried out the analysis with a general convection term.

The structure of this paper is as follows: In Section 2, we relate the analytical solution bound of the system of equations with the solution bound of a scalar convection-diffusion BVP and provide a stability bound of the solution. Bounds for the derivatives of the continuous solution are also provided. Then, in Section 3, we outline the numerical discretization of (1.1) using the upwind finite difference scheme, with a discrete stability bound. The main result, first-order uniform convergence using the proposed monitor function is derived here using the discrete l_∞ norm, from a sufficient condition of uniform convergence. In Section 4, a semi-linear convection-diffusion system of BVPs is introduced. Numerical results using an adaptive algorithm are given in Section 5, to show that the rate of convergence predicted by our analysis holds true in practice. Finally in Section 6, we make a concise conclusion.

Notation. Throughout this paper C, denotes a generic positive constant independent of the grid points x_i and the parameters ε_k and N (the number of mesh intervals) which may take different values at different places. For any mesh function $\{\phi_i\}_{i=0}^N$ defined on a nonuniform mesh Ω^N, we define the following norms

$$\|\phi\| = \max_{\overline{\Omega}} |\phi(x)|, \qquad \|\Phi\| = \max_{1\le i\le k} |\phi_i(x)| \text{ where } \Phi = (\phi_1,\phi_2,\cdots,\phi_k)^T.$$

Another discrete norm defined by

$$||v||_{-1,\infty,\Omega^N} = \min_{\gamma\in R}\max_{i=0,\cdots,N-1}\left|\sum_{j=i}^{N-1} h_{j+1}v_j - \gamma\right|, \tag{1.5}$$

will be used for our later analysis. Here $h_i = x_i - x_{i-1}$. Whenever we write $\phi = \mathcal{O}(\psi)$, we mean that $|\phi| \le C|\psi|$. To simplify the notation, we set $g_i = g(x_i)$ for any function g, while G_i or G_i^N denote a discrete approximation of g at x_i.

2. CONTINUOUS PROBLEM AND SOLUTION BOUNDS

This section provides the stability property of the analytical solution $\boldsymbol{u}$ of (1.1). We start by recalling the stability of the scalar convection-diffusion BVP, which is used to derive the stability of the solution $\boldsymbol{u}$. The following lemma (see for *e.g.,* [11]) provides the stability estimate of the general scalar BVP.

Lemma 2.1. *Assume the coefficients of the following SPP*

$$\begin{cases} -\varepsilon u'' - a(x)u' + b(x)u = f(x), & \textit{for} \quad x\in\Omega, \\ u(0)=u(1)=0, \end{cases} \tag{2.1}$$

satisfies $a(x), b(x), f(x) \in \mathcal{C}(\Omega)$ *with* $\varepsilon > 0, a(x) \geq \alpha > 0, b(x) \geq \beta > 0$ *for all* $x \in \overline{\Omega}$. *Then, for any* $u \in \mathcal{C}^2(\Omega) \cap \mathcal{C}(\overline{\Omega})$, *we have the following stability estimate*

$$||u|| \leq \min\left\{\left\|\frac{f}{a}\right\|, \left\|\frac{f}{b}\right\|\right\}.$$

Now, with the help of above lemma the stability for each component of $\boldsymbol{u}$ is addressed here.

Lemma 2.2. *Let* $\boldsymbol{u}$ *be the solution of (1.1) and assume that the coupling matrix* $\boldsymbol{B}$ *satisfy the* L_0*-matrix condition (1.2). Then*

$$||u_m|| \leq \sum_{l=1}^{k} (\Upsilon^{-1})_{ml} \min\left\{\left\|\frac{f_l}{a_{ll}}\right\|, \left\|\frac{f_l}{b_{ll}}\right\|\right\},$$

where the $k \times k$ *matrix* $\Upsilon = \Upsilon(\boldsymbol{A},\boldsymbol{B}) = (\gamma_{ml})_{k\times k}$ *is such that*

$$\gamma_{ml} = -\min\left\{\left\|\frac{b_{ml}}{b_{mm}}\right\|, \left\|\frac{b_{ml}}{a_{mm}}\right\|\right\}, \text{ for } m \neq l \text{ and } \gamma_{mm} = 1.$$

Proof. A single equation from the system of BVPs (1.1) can be written as

$$-\varepsilon_m u_m'' - a_{mm} u_m' + b_{mm} u_m = f_m - \sum_{l=1, l\neq m}^{k} b_{ml} u_l, \text{ for } m = 1, \cdots, k. \tag{2.2}$$

Under the condition of L_0-matrix, Lemma 2.1 yields

$$||u_m|| - \sum_{l=1, l\neq m}^{k} \min\left\{\left\|\frac{b_{ml}}{b_{mm}}\right\|, \left\|\frac{b_{ml}}{a_{mm}}\right\|\right\} ||u_l|| \leq \min\left\{\left\|\frac{f_m}{a_{mm}}\right\|, \left\|\frac{f_m}{b_{mm}}\right\|\right\}, \ m = 1, \cdots, k.$$

Now define a $k \times k$ matrix $\Upsilon = \Upsilon(\boldsymbol{A}, \boldsymbol{B}) = (\gamma_{ml})_{k\times k}$ such that

$$\gamma_{ml} = -\min\left\{\left\|\frac{b_{ml}}{b_{mm}}\right\|, \left\|\frac{b_{ml}}{a_{mm}}\right\|\right\}, \text{ for } m \neq l \text{ and } \gamma_{mm} = 1.$$

If we assume Υ to be inverse monotone *i.e.*, $\Upsilon^{-1} \geq 0$, then

$$||u_m|| + \sum_{l=1, l\neq m}^{k} \gamma_{ml} ||u_l|| \leq \min\left\{\left\|\frac{f_m}{a_{mm}}\right\|, \left\|\frac{f_m}{b_{mm}}\right\|\right\}, \ m = 1, \cdots, k.$$

The matrix $\boldsymbol{B}$ is assumed to be an L_0-matrix from (1.2). Therefore, Υ will be inverse monotone. Hence, we get the required stability bound. ∎

As a consequence the stability of the continuous solution $\boldsymbol{u}(x)$ can be obtained. It should be noted that, one can directly compute the inverse of the matrix Υ from the definition of Υ. Its sign pattern for the condition of inverse monotonicity can also be checked. Therefore, in order to get the stable solution of (1.1), the L_0-matrix condition is not necessary for the matrix $\boldsymbol{B}$.

The following theorem provides the derivative estimates of the solution $\boldsymbol{u}$.

Theorem 2.3. *Under the assumptions from (1.2), the solution* $\boldsymbol{u}$ *of the system (1.1) and its derivatives satisfy the following bounds for* $x \in \overline{\Omega}$,

$$|u_m^{(n)}| \leq C\left[1 + \varepsilon_m^{-n} \exp\left(-\frac{\alpha_m x}{\varepsilon_m}\right)\right], \text{ where } a_{mm}(x) \geq \alpha_m, \text{ for } n = 0, 1,$$

and

$$|u_m^{(2)}| \leq C\left[1 + \sum_{p=1}^{k} \varepsilon_p^{-2} \exp\left(-\frac{\alpha_p x}{\varepsilon_p}\right)\right], \text{ where } a_{pp}(x) \geq \alpha_p, \text{ for } m, p = 1, \cdots, k.$$

Proof. The bounds of the solution $\boldsymbol{u}$ and its first-order derivative are given by Linß [10], where a standard technique, provided in Kellog and Tsan [9] for scalar operators is used. The proof provided in Zhongdi [13] for two equations can be extended to bound the second-order derivative of the solution of the system (1.1). ∎

3. Numerical Scheme and Nonuniform Grids

This section is devoted for the discretization of the continuous problem. The monitor function is obtained through the error analysis, which can be equidistributed to get parameter uniform convergence.

3.1. **Discrete problem.** Here, we shall consider the finite difference approximation of (1.1) on a nonuniform grid $\Omega^N \equiv \{0 = x_0 < x_1 < \cdots < x_N = 1\}$ with the step sizes $h_i = x_i - x_{i-1},\ i = 1, \cdots, N$. Given a discrete function $\{v_i\}_{i=0}^N$, define the forward and backward difference operators

$$D^+ v_i = \frac{v_{i+1} - v_i}{h_{i+1}}, \quad \text{and} \quad D^- v_i = \frac{v_i - v_{i-1}}{h_i},$$

respectively, where $\hbar_i = (h_i + h_{i+1})/2$. Let $\boldsymbol{U}$ be the discrete approximation of the continuous solution $\boldsymbol{u}(x)$. Then, by denoting $\boldsymbol{U}_i = \boldsymbol{U}(x_i)$, the discretized problem of (1.1) is defined as follows:

$$\begin{cases} \text{Find } \boldsymbol{U}_1, \cdots, \boldsymbol{U}_{N-1} \text{ satisfying} \\ [\mathbf{L}^N \boldsymbol{U}]_i = \boldsymbol{f}_i, \quad \text{for} \quad i = 1, 2, \cdots, N-1, \\ \boldsymbol{U}_0 = \boldsymbol{U}_N = 0, \end{cases}$$

i.e., find $U_{m,1}, \cdots, U_{m,N-1}$, for $m = 1, \cdots, k$ satisfying

$$\begin{cases} [\mathbf{L}_m^N \boldsymbol{U}]_i \equiv [\Lambda_m^N U_m]_i + \sum_{l=1, l\neq m}^k b_{ml} U_{l;i} = f_{m;i}, \quad \text{with} \quad i = 1, 2, \cdots, N-1, \\ U_{m,0} = U_{m,N} = 0, \end{cases} \tag{3.1}$$

where $\mathbf{L}^N = (\mathbf{L}_1^N, \mathbf{L}_2^N, \cdots, \mathbf{L}_k^N)^T$ is the discrete analogue of $\mathbf{L}$ and

$$[\Lambda_m^N v]_i \equiv -\varepsilon_m D^+ D^- v_i - a_{mm;i} D^+ v_i + b_{mm;i} v_i.$$

In a similar way, if a_{mm} is negative, then the upwind scheme will be defined as

$$[\Lambda_m^N v]_i \equiv -\varepsilon_m D^- D^+ v_i - a_{mm;i} D^- v_i + b_{mm;i} v_i.$$

The discrete solution satisfies the following stability result (see for *e.g.*, [1, 10]).

Lemma 3.1. *Under the L_0-matrix condition, we have*

$$||v||_{\Omega^N} \leq \left\| \frac{\Lambda_m^N v}{b_{mm}} \right\|_{\Omega^N}, \ \textit{for } v \in \mathbb{R}^{N+1},$$

and

$$||v||_{\Omega^N} \leq C ||\Lambda_m^N v||_{-1,\infty,\Omega^N} = C \min_{V: D^+ V = \Lambda_m^N v} ||V||_{\Omega^N}. \tag{3.2}$$

Let $\boldsymbol{E} = \boldsymbol{u} - \boldsymbol{U}$ be the error of the discrete solution obtained by the finite difference scheme (3.1), where $E_{m,i} = u_{m,i} - U_{m,i},\ m = 1(1)k,\ i = 0(1)N$, ***i.e.***, $\boldsymbol{E} \in (\mathbb{R}^{N+1})^k$. We divide the error $\boldsymbol{E}$ in two components $\aleph$, $\Re$ such that $\boldsymbol{E} = \aleph + \Re$ satisfies

$$[\Lambda_m^N \aleph_m]_i = [\mathbf{L}_m^N (\boldsymbol{U} - \boldsymbol{u})]_i, \quad i = 1, 2, \cdots, N-1, \quad \aleph_{m,0} = \aleph_{m,N} = 0, \quad m = 1, 2, \cdots, k, \tag{3.3}$$

and
(3.4)
$$[\Lambda_m^N \Re_m]_i = -\sum_{l=1, l\neq m}^{k} b_{ml,i} E_{l,i}, \quad i = 1, 2, \cdots, N-1, \quad \Re_{m,0} = \Re_{m,N} = 0, \quad m = 1, 2, \cdots, k.$$
From Lemma 3.1, it follows that
$$||E_m||_{\Omega^N} \leq ||\aleph_m||_{\Omega^N} + ||\Re_m||_{\Omega^N} \leq ||\aleph_m||_{\Omega^N} + \sum_{l=1, l\neq m}^{k} \left\| \frac{b_{ml}}{b_{mm}} \right\|_{\Omega^N} ||E_l||_{\Omega^N}, \quad m = 1, 2, \cdots, k,$$
which leads to
$$||\boldsymbol{U} - \boldsymbol{u}||_{\Omega^N} \leq C||\aleph||_{\Omega^N}. \tag{3.5}$$
Now, using the stability inequality from Lemma 3.1 for the discrete solution and the solution bound from Theorem 2.3, it is easy to derive the following lemma.

Lemma 3.2. *The solution of (3.3) i.e., the components $\aleph_m$ of the term $\aleph$ satisfy*
$$||\aleph_m||_{\Omega^N} \leq C \max_{i=1,\cdots,N} \int_{x_{i-1}}^{x_i} \left[1 + \sum_{m=1}^{k} |u_m'(x)| \right] dx,$$
where C is independent of the perturbation parameters ε_m and the number of mesh intervals N.

Proof. This result is proved in Linß [10]. ∎

Hence, the inequality (3.5) reduces to the following result.

Theorem 3.3. *Let $\boldsymbol{u}$ be the solution of the system (1.1) and $\boldsymbol{U}$ be the finite difference approximate solution of (3.1), then we have*
$$||\boldsymbol{u} - \boldsymbol{U}||_{\Omega^N} \leq C \max_{i=1,\cdots,N} \int_{x_{i-1}}^{x_i} \left[1 + \sum_{m=1}^{k} |u_m'(x)| \right] dx,$$
where C is independent of the perturbation parameters ε_m and the number of mesh intervals N.

The next theorem provides a sufficient condition for choosing an appropriate monitor function, whose equidistribution will lead to the layer-adapted mesh.

Theorem 3.4. *Assume that there exist positive constants C_1, C_2 and C_3 independent of the perturbation parameters ε_m, such that a monitor function $M(x, \boldsymbol{u}(x))$ satisfies*
$$\int_{x_{i-1}}^{x_i} \left[1 + \sum_{m=1}^{k} |u_m'(x)| \right] dx \leq C_1 \int_{x_{i-1}}^{x_i} M(x, \boldsymbol{u}(x)) dx, \text{ for } i = 1, \cdots, N, \tag{3.6}$$
$$\int_0^1 M(x, \boldsymbol{u}(x)) dx \leq C_2, \tag{3.7}$$
and
$$M(x, \boldsymbol{u}(x)) \geq C_3. \tag{3.8}$$
Then
$$||\boldsymbol{U} - \boldsymbol{u}||_{\Omega^N} \leq CN^{-1},$$
where C is independent of the perturbation parameters ε_m and the number of mesh intervals N.

Proof. Note that from the definition of equidistribution principle (1.4), we have

$$C_3 h_i \le \int_{x_{i-1}}^{x_i} M(x,\boldsymbol{u}(x))dx = \frac{1}{N}\int_0^1 M(x,\boldsymbol{u}(x))dx \le C_2 N^{-1}$$

which implies that

$$h_i \le C_2 C_3^{-1} N^{-1}.$$

Now using (3.6)-(3.8) with the equidistribution principle (1.4), we obtain

$$\begin{aligned} ||\aleph_m||_{\Omega^N} &\le C \max_i \int_{x_{i-1}}^{x_i} \left[1+\sum_{m=1}^{k}|u_m'(x)|\right]dx \\ &\le C\int_{x_{i-1}}^{x_i} M(x,\boldsymbol{u}(x))dx \le CN^{-1}\int_0^1 M(x,\boldsymbol{u}(x))dx \le CN^{-1}. \end{aligned}$$

Hence, the inequality (3.5) leads to

$$||\boldsymbol{U}-\boldsymbol{u}||_{\Omega^N} \le CN^{-1}.$$

■

Now consider the following monitor function

$$M(x,\boldsymbol{u}(x)) = 1+\sum_{m=1}^{k}|u_m''|^{1/2}. \tag{3.9}$$

This monitor function is a generalized form of the monitor function proposed by Beckett and Mackenzie [2] for a scalar case of (1.1), where the solution u is decomposed into two components, the so called smooth component v and the singular component w. In reality, from the *apriori* analysis, it is observed that the boundary layer phenomena occurs actually from the singular component of the solution. It should also be noted that the second-order derivative of the smooth component v is bounded. These facts motivate them to consider a monitor function involving especially derivative of the singular component. This monitor function also works well for reaction-diffusion type problems [3].

Now, our aim is to show that the monitor function given in (3.9) satisfies all conditions of Theorem 3.4. To show this, observe that Theorem 2.3 with $\alpha = \min_m \alpha_m$ implies

$$\begin{aligned} |u_m''(x)|^{1/2} &\le C\left[1+\sum_{p=1}^{k}\varepsilon_p^{-2}\exp\left(-\frac{\alpha x}{\varepsilon_p}\right)\right]^{1/2} \\ &\le C\left[\max\left(1,\varepsilon_p^{-2}\exp\left(-\frac{\alpha x}{\varepsilon_p}\right)\right)\right]^{1/2}, \text{ for } p=1,2,\cdots,k, \end{aligned}$$

where we have used the fact that for any n positive functions $g_1, g_2, \cdots, g_n$, we get

$$\left(\sum_{p=1}^{n} g_p\right)^{1/2} \le \sqrt{n}\left[\max_p(g_p)\right]^{1/2}.$$

Note that

$$\int_0^1 \left[\varepsilon_p^{-2}\exp\left(-\frac{\alpha x}{\varepsilon_p}\right)\right]^{1/2}dx = \frac{\alpha}{2}\left[1-\exp\left(-\frac{\alpha}{2\varepsilon_p}\right)\right] < \beta_p \quad \text{(say)}.$$

Therefore, we have

$$\int_0^1 M(x,\boldsymbol{u}(x))dx \le \max(1,\beta_p) = C_2 \quad \text{(say)}.$$

Thus the condition (3.7) is satisfied. Now, from the equation (2.2), we have

$$u_m' = \frac{1}{a_{mm}}\Big[-\varepsilon_m u_m'' + \sum_{l=1}^{k} b_{ml} u_l - f_m \Big].$$

Hence, it follows from Lemma 2.2 that

$$|u_m'| \le C[\varepsilon_m |u_m''| + 1].$$

Thereafter, it is enough to show that

$$\sum_{m=1}^{k} \varepsilon_m |u_m''| \le C \sum_{m=1}^{k} |u_m''|^{1/2}.$$

From the given equation (2.2), we can write

$$|\varepsilon_m u_m^{''}| \le C\Big[1 + \varepsilon_m^{-1} \exp\Big(\frac{-\alpha_m x}{\varepsilon_m}\Big)\Big]. \tag{3.10}$$

Now we shall show that $\varepsilon_m |u_m''| \le C |u_m''|^{1/2}$. Assuming that $u_m'' \neq 0$, the inequality (3.10) leads to

$$\begin{aligned} |\varepsilon_m u_m''|^{1/2} &\le C\Big[1 + \varepsilon_m^{-1} \exp\Big(-\frac{\alpha_m x}{\varepsilon_m}\Big)\Big]^{1/2} \\ &\le \sqrt{2} C\Big[\max\Big(1, \varepsilon_m^{-1} \exp\Big(-\frac{\alpha_m x}{\varepsilon_m}\Big)\Big)\Big]^{1/2}. \end{aligned}$$

Thus, we have

$$\varepsilon_m |u_m''|^{1/2} \le C\sqrt{\varepsilon_m}\Big[\max\Big(1, \varepsilon_m^{-1} \exp\Big(-\frac{\alpha_m x}{\varepsilon_m}\Big)\Big)\Big]^{1/2} \le C.$$

That is,

$$\varepsilon_m |u_m''| \le C |u_m''|^{1/2}.$$

Therefore, we obtain that

$$\begin{aligned} ||\aleph_m||_{\Omega^N} &\le C \max_{i=1,\cdots,N} \int_{x_{i-1}}^{x_i} \Big[1 + \sum_{m=1}^{k} |u_m'(x)|\Big] dx \\ &\le C \max_{i=1,\cdots,N} \int_{x_{i-1}}^{x_i} \Big[1 + \sum_{m=1}^{k} \varepsilon_m |u_m''(x)|\Big] dx \\ &\le C \max_{i=1,\cdots,N} \int_{x_{i-1}}^{x_i} \Big[1 + \sum_{m=1}^{k} |u_m''(x)|^{1/2}\Big] dx, \end{aligned}$$

i.e.,

$$\max_{i=1,\cdots,N} \int_{x_{i-1}}^{x_i} \Big[1 + \sum_{m=1}^{k} |u_m'(x)|\Big] dx \le C \int_{x_{i-1}}^{x_i} M(x, \boldsymbol{u}(x)) dx.$$

Again, we have

$$1 \le M(x, \boldsymbol{u}(x)).$$

Thus, conditions (3.6) and (3.8) are satisfied. Hence, Theorem 3.4 implies that

$$||\boldsymbol{U} - \boldsymbol{u}||_{\Omega^N} \le C N^{-1}.$$

Now, we state the main result of this paper.

Theorem 3.5. *Let* $\boldsymbol{u}$ *be the solution of the system (1.1) and* $\boldsymbol{U}$ *be the numerical solution of the corresponding discretized problem (3.1), on the mesh* Ω^N*, which is obtained by equidistributing the monitor function (3.9). Then there exists a constant C, independent of* N *and* ε*, such that*

$$\|\boldsymbol{u}-\boldsymbol{U}\|_{\Omega^N} \leq CN^{-1}.$$

4. Semilinear convection-diffusion System

Consider the following singularly perturbed system of semilinear convection-diffusion BVPs:

$$\begin{cases} \mathrm{L}\boldsymbol{u} \equiv -\boldsymbol{Eps}\,\boldsymbol{u}_{xx}(x) - \boldsymbol{A}(x)\boldsymbol{u}_x(x) + \boldsymbol{f}(x,\boldsymbol{u}(x)) = 0, \quad \text{for} \quad x \in \Omega, \\ \boldsymbol{u}(0) = \boldsymbol{u}(1) = 0, \end{cases} \tag{4.1}$$

where $\boldsymbol{f}(x,\boldsymbol{u}) = (f_1(x,\boldsymbol{u}),\cdots,f_k(x,\boldsymbol{u}))^T$. Here, $f_m(x,\boldsymbol{u})$ can involve nonlinear terms of $\boldsymbol{u}$ and the notations $\boldsymbol{u}_x$, $\boldsymbol{u}_{xx}$ are used instead of $\boldsymbol{u}'$ and $\boldsymbol{u}''$ respectively, for the sake of convenience. We shall assume that

$$\frac{\partial f_m}{\partial u_l}(x,\boldsymbol{u}) \leq 0, \quad m \neq l, \quad \sum_{l=1}^{k} \frac{\partial f_m}{\partial u_l}(x,\boldsymbol{u}) \geq \beta > 0, \quad m = 1\cdots,k, \tag{4.2}$$

on $(x,\boldsymbol{u}) \in \overline{\Omega} \times \mathbb{R}^k$. Assume that the reduced problem, which is obtained by setting $\mathbf{Eps} = \mathbf{0}$ in (4.1), has a unique solution in $\overline{\Omega}$. Under this assumption, the system of BVP (4.1) admits a unique solution in $\overline{\Omega}$. Chang and Howes [6] studied the theoretical aspects corresponding to the semilinear system of convection-diffusion problems.

To obtain the numerical solution of the system (4.1), the well-known Newton's quasilinearization technique is used. This technique allows us to linearize the system into a sequence of linear problems, whose solutions $\boldsymbol{u}^{(p)}$ with a proper initial guess $\boldsymbol{u}^{(0)}$ will converge to the original solution $\boldsymbol{u}$. For each fixed nonnegative integer p, define $\boldsymbol{u}^{(p+1)}$ to be the solution of the linear problem

$$\begin{cases} \overline{\mathrm{L}}\boldsymbol{u}^{(p+1)} \equiv -\boldsymbol{Eps}\,\boldsymbol{u}^{(p+1)}_{xx}(x) - \boldsymbol{A}(x)\boldsymbol{u}^{(p+1)}_x(x) + \boldsymbol{J}(x)\boldsymbol{u}^{(p+1)}(x) = \boldsymbol{F}(x,\boldsymbol{u}^{(p)}(x)), \quad \text{for } x \in \Omega, \\ \boldsymbol{u}^{(p+1)}(0) = \boldsymbol{u}^{(p+1)}(1) = 0, \end{cases} \tag{4.3}$$

for $p = 0,1,\cdots$. Here $\boldsymbol{J}(x)$ is the Jacobian matrix which is given by

$$\boldsymbol{J}(x) = \begin{pmatrix} \dfrac{\partial f_1(x,\boldsymbol{u}^{(p)})}{\partial u_1} & \cdots & \dfrac{\partial f_1(x,\boldsymbol{u}^{(p)})}{\partial u_k} \\ \vdots & \ddots & \vdots \\ \dfrac{\partial f_k(x,\boldsymbol{u}^{(p)})}{\partial u_1} & \cdots & \dfrac{\partial f_k(x,\boldsymbol{u}^{(p)})}{\partial u_k} \end{pmatrix}_{k\times k},$$

and $\boldsymbol{F}(x,\boldsymbol{u}^{(p)}) = \boldsymbol{J}(x)\boldsymbol{u}^{(p)}(x) - \boldsymbol{f}(x,\boldsymbol{u}^{(p)}(x))$. It is easy to see that the Jacobian matrix $\boldsymbol{J}(x)$ satisfies all the conditions of an L_0- matrix defined in (1.2). If the initial guess $\boldsymbol{u}^{(0)}$ is sufficiently close to the solution $\boldsymbol{u}$, then following the proof given in Doolan et. al. [8], one can show that the sequence $\boldsymbol{u}^{(p+1)}$ converges to the solution $\boldsymbol{u}$. The solution of the associated reduced problem can be taken as an initial guess $\boldsymbol{u}^{(0)}(x)$. Since, for each fixed p the system (4.3) is a linear system of the form (1.1), the mesh generation procedure by equidistributing the proposed monitor function explained in Section 3 can be applied to generate a layer-adapted mesh. The obtained solutions will converge uniformly to the continuous solution as p increases. We use the following criteria

$$|\boldsymbol{u}^{(p+1)}(x_i) - \boldsymbol{u}^{(p)}(x_i)| \leq Tol, \quad x_i \in \overline{\Omega}, \quad p \geq 0,$$

for convergence of the iterative quasi-linearization technique. Here, *Tol* denotes the user chosen tolerance bound.

5. Numerical Experiments

The generation of the adaptive finite difference solution requires two steps; firstly the adaptive mesh has to be determined by a mesh generation algorithm and thereafter, the finite difference solution has to be computed on that mesh. To generate the adaptive mesh, we use the monitor function given in (3.9).

5.1. **Practical Implementation –Adaptive Algorithm.**

Here, we shall use the following iterative algorithm for generating the new mesh by equidistributing the proposed monitor function. This algorithm is applied for scalar SPP by Chadha and Kopteva in [5] with the convergence analysis.

Here our aim is to construct a mesh that solves the following equidistribution problem

$$M_i h_i = \frac{1}{N}\sum_{j=1}^{N} M_j h_j, \quad \text{for} \quad i = 1, \cdots, N,$$

where M_i is the discrete approximation of the monitor function $M(x, \boldsymbol{u}(x))$ at the subinterval (x_{i-1}, x_i). Observe that instead of solving the discretized equidistribution problem (1.4) exactly, it is sufficient that this algorithm can be stopped when the weakly equidistribution principle

$$M_i h_i \leq \frac{C_0}{N}\sum_{j=1}^{N} M_j h_j, \quad \text{for} \quad i = 1, \cdots, N,$$

satisfied with a user chosen constant $C_0 > 1$. The constant C_0 will be chosen larger enough to obtain the convergence in a fewer iterations. When C_0 approaches 1, this algorithm results in more accurate solution with many iterations.

5.1.1. *Algorithm-.*

Step 1: Define the initial uniform mesh $\{x^{(0)} : 0 \leq i \leq N,\ x_i^{(0)} = i/N\}$ and go to Step-2 with $p = 0$.

Step 2: Solve $\mathbf{L}^N \boldsymbol{U}_i^{(p)} = \boldsymbol{f}_i^{(p)}$ with $\boldsymbol{U}_0^{(p)} = \boldsymbol{u}(0)$ and $\boldsymbol{U}_N^{(p)} = \boldsymbol{u}(1)$ at the mesh $\{x_i^{(p)} : 0 \leq i \leq N\}$ for $\boldsymbol{U}_i^{(p)} = (U_{1,i}^{(p)}, \cdots, U_{k,i}^{(p)})$ and define $h_{i+1}^{(p)} = x_{i+1}^{(p)} - x_i^{(p)}$.

Step 3: Find the discretized monitor function at the ith interior node

$$\phi_i^{(p)} = \left[1 + \sum_{m=1}^{k} |D^2 U_{m,i}^{(p)}|^{1/2}\right], \text{ for } i = 1, \cdots, N-1,$$

where $D^2 = D^+D^-$. Define $\hat{\phi}_i = (\phi_i^{(p)} + \phi_{i-1}^{(p)})/2$ for $i = 1, \cdots, N$, by setting $\phi_0^{(p)} = \phi_1^{(p)}$ and $\phi_N^{(p)} = \phi_{N-1}^{(p)}$. Compute

$$\Phi_j^{(p)} = \sum_{i=1}^{j} h_i^{(p)} \hat{\phi}_i^{(p)}.$$

Step 4: Choose a constant $C_0 > 1$. The stopping criteria for the iterative technique is

$$\frac{\max_{i=1,\ldots,N} h_i^{(p)} \hat{\phi}_i^{(p)}}{\Phi_N^{(p)}} \leq \frac{C_0}{N}.$$

If it holds true, then go to Step-6, else continue with Step-5.

Step 5: Generate a new mesh by equidistributing the proposed monitor function using current computed solution from Step-2 and $\Phi_j^{(p)}$ from Step-3: Set $Y_i^{(p)} = i\Phi_N^{(p)}/N$ for $i = 0, \cdots, N$. Now interpolate $(Y_i^{(p)}, x_i^{(p+1)})$ to $(\Phi_i^{(p)}, x_i^{(p)})$ using piecewise linear interpolation. Generate a new mesh $x^{(p+1)} \equiv \{0 = x_0^{(p+1)} < x_1^{(p+1)} < \cdots < x_N^{(p+1)} = 1\}$ and return to Step-2.

Step 6: Set $x^* = \{0 = x_0^* < x_1^* < \cdots < x_N^* = 1\} = x^{(p+1)}$ and $\boldsymbol{U}^* = \boldsymbol{U}^{(p+1)}$, where $\boldsymbol{U}^*$ is our desired solution. Stop.

In order to highlight the results of our theoretical findings and to numerically study the various components of the error estimator, we supply three test problems. For these three test problems, the maximum point-wise errors and the corresponding rates of convergence are highlighted through tables.

Example 5.1. *Consider the following system of singularly perturbed BVPs:*

$$\begin{cases} -\varepsilon_1 u_1''(x) - u_1'(x) + 2u_1(x) - u_2(x) = f_1(x), \quad x \in (0,1), \\ -\varepsilon_2 u_2''(x) - 2u_2'(x) - u_1(x) + 4u_2(x) = f_2(x), \\ u_1(0) = u_1(1) = u_2(0) = u_2(1) = 0, \end{cases}$$

where $f_1(x)$ and $f_2(x)$ are chosen such a way, that the exact solution is given by

$$\begin{cases} u_1(x) = \dfrac{1-\exp(-x/\varepsilon_1)}{1-\exp(-1/\varepsilon_1)} + \dfrac{1-\exp(-x/\varepsilon_2)}{1-\exp(-1/\varepsilon_2)} - 2\sin\dfrac{\pi}{2}x, \\ u_2(x) = \dfrac{1-\exp(-x/\varepsilon_2)}{1-\exp(-1/\varepsilon_2)} - x\exp(x-1). \end{cases}$$

For any value of N and $\varepsilon = (\varepsilon_1, \varepsilon_2)$, we calculate the exact maximum point-wise errors $E_{m,\varepsilon}^N$ for the solution components u_m, $m = 1, 2$, by

$$E_{m,\varepsilon}^N = \max_{0 \le i \le N} |u_m(x_i) - U_{m,i}^N|,$$

where $u_m(x_i)$ is the exact solution and $U_{m,i}^N$ is the numerical solution at the mesh point x_i, obtained by using N number of mesh intervals in the domain Ω^N.

The uniform errors for each fixed N, are defined by taking the maximum over wide range of ε, say from the set S, namely

$$E_m^N = \max_{\varepsilon \in S} E_{m,\varepsilon}^N,$$

and the corresponding parameter uniform rates of convergence is calculated by the following formula

$$r_m^N = \log_2\left(\frac{E_m^N}{E_m^{2N}}\right).$$

The second problem considered here, has boundary layers at both the ends.

Example 5.2. *Consider the following system of convection-diffusion problem:*

$$\begin{cases} -\varepsilon_1 u_1''(x) + (5 - x^2)u_1'(x) + (4+x)u_1(x) - u_2(x) = 2\exp(x), \quad x \in (0,1), \\ -\varepsilon_2 u_2''(x) - 6u_2'(x) - 2u_1(x) + (4-x)u_2(x) = 10x + 1, \\ u_1(0) = u_1(1) = u_2(0) = u_2(1) = 0. \end{cases}$$

Our next problem is a system of semilinear convection-diffusion equations.

Example 5.3. *Consider the system of semilinear SPPs:*

$$\begin{cases} -\varepsilon_1 u_1'' - 2(x+1)^2 u_1' + u_1 - 1 - (1-u_1)^3 + \exp(u_1 - u_2) = 0, \quad x \in (0,1), \\ -\varepsilon_2 u_2'' - 5u_2' + u_2 - 0.5 - (0.5 - u_2)^5 + \exp(u_2 - u_1) = 0, \\ u_1(0) = u_1(1) = u_2(0) = u_2(1) = 0. \end{cases}$$

Exact solutions for the Example 5.2 and Example 5.3 are not available. So the accuracy of their numerical solutions will be computed using double mesh principle. For any value of N, the maximum pointwise errors $E_{m,\varepsilon}^N$ for the solution u_m, $m = 1, 2$, will be calculated by

$$E_{m,\varepsilon}^N = \max_{0 \le i \le N} |U_m^N - \overline{U}_{m,i}^{2N}|,$$

where U_m^N is the computed solution with N number of mesh intervals and $\overline{U}_m^{2N}$ is the numerical solution on a mesh, obtained by bisecting the original mesh with N number of mesh intervals.

The uniform errors for each fixed N and the corresponding parameter uniform rates of convergence are calculated by the same formula as for the previous example.

For the numerical experiments of all the test problems, we take ε_1 and ε_2 from the set

$$S = \{\varepsilon = (\varepsilon_1, \varepsilon_2) | \varepsilon_1 = 1, 2^{-2}, \cdots, 2^{-22}; \varepsilon_2 = 1, 2^{-2}, \cdots, 2^{-22}\},$$

and in the numerical computation, we equidistribute (3.9) by taking $C_0 = 3$.

In Tables 5.1 and 5.2, we present the uniform errors and the corresponding orders of convergence for the solution components u_1 and u_2 respectively of Example 5.1, which clearly indicate that the proposed method is ε-uniform first-order accurate. The same behaviour is also observed for Example 5.2 from Tables 5.3 and 5.4. These tables demonstrate the uniform errors and the corresponding first-order convergence to the solution components u_1 and u_2 respectively, where double mesh principle is used to calculate the errors and the rates of convergence.

To show the effectiveness of our proposed monitor function numerically, we solve a system of semilinear convection-diffusion BVPs in Example 5.3 with $Tol = 10^{-8}$. The numerical results, that is, the uniform errors and orders of convergence given in Tables 5.5 and 5.6 for Example 5.3 support the theoretical estimates.

In Figure 1 and Figure 2, we display the error plots for Example 5.1 and 5.2 respectively. These two figures show that the maximum errors occur only in boundary layers regions. Mesh points are also dense in these regions. In Figure 3 and Figure 4, the maximum point-wise errors versus number of mesh intervals are plotted for the Example 5.2 and Example 5.3, respectively. These figures are drawn in logarithmic scale for $\varepsilon_1 = 2^{-12}$, $\varepsilon_2 = 2^{-16}$ and $\varepsilon_1 = 2^{-22}$, $\varepsilon_2 = 2^{-16}$ respectively. Graphically these also suggest that the computed errors are decreasing with the rate of $O(N^{-1})$ as the number of interval N increases.

Table 5.1: Uniform errors and orders for u_1 for Example 5.1.

$(\varepsilon_1, \varepsilon_2) \in S$	Number of intervals N						
	64	128	256	512	1024	2048	4096
E_1^N	3.5643e-1	1.3102e-1	5.1964e-2	2.4510e-2	1.1505e-2	5.7534e-3	2.8699e-3
r_1^N	1.4438	1.3343	1.0842	1.0911	0.9998	1.0034	-

The advantage of generating the meshes by the adaptive technique is that it does not require any *apriori* knowledge about the location and widths of the boundary layers. This technique leads to an optimal parameter uniform convergence corresponding to the upwind discretization, by equidistributing the proposed monitor function.

Table 5.2: Uniform errors and orders for u_2 for Example 5.1.

$(\varepsilon_1, \varepsilon_2) \in S$	Number of intervals N						
	64	128	256	512	1024	2048	4096
E_2^N	1.5564e-1	6.2899e-2	2.1974e-2	1.0940e-2	5.0224e-3	2.4649e-3	1.2174e-3
r_2^N	1.3071	1.5172	1.0063	1.1231	1.0269	1.0177	-

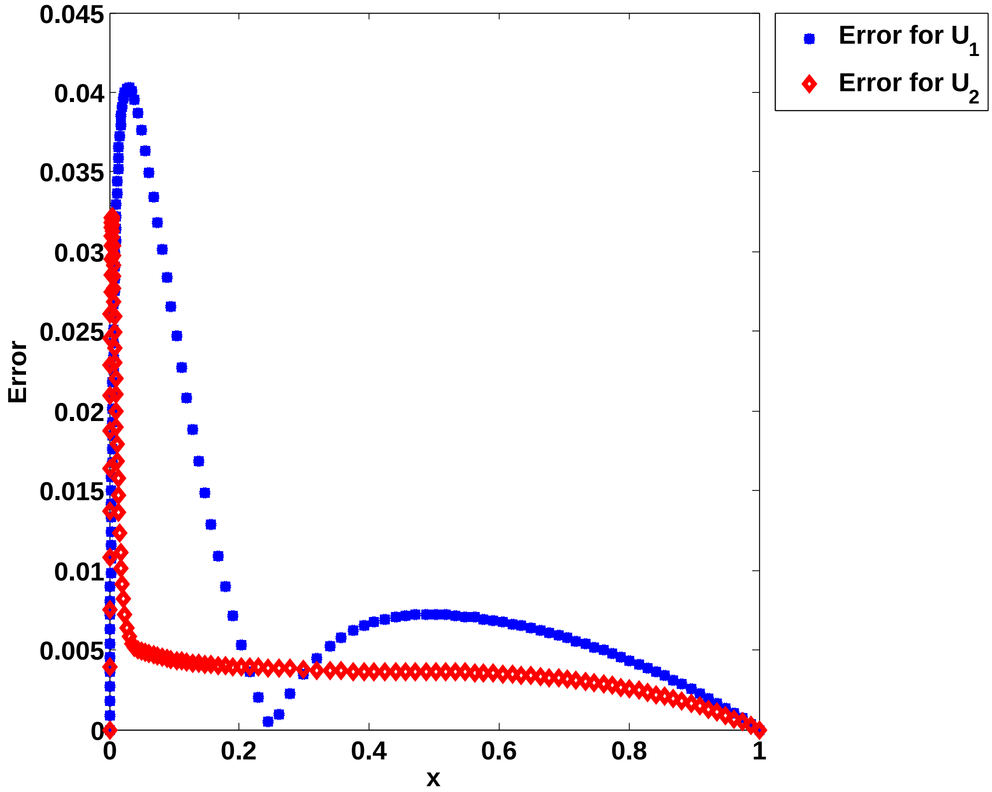

Figure 1: Error plot for U_1 and U_2 with $N = 128$ to the Example 5.2.

Table 5.3: Uniform errors and orders for u_1 for Example 5.2.

$(\varepsilon_1, \varepsilon_2) \in S$	Number of intervals N						
	64	128	256	512	1024	2048	4096
E_1^N	7.2515e-2	3.2051e-2	1.4278e-2	5.6939e-3	2.9827e-3	1.3425e-3	6.3003e-4
r_1^N	1.1779	1.1666	1.3263	0.93282	1.1517	1.0914	-

6. Conclusion and discussion

In this article, we present the analysis for the discretization of singularly perturbed weakly coupled system of BVPs of the form (1.1) by using upwind finite difference scheme. The numerical solution is obtained on a suitable layer-adapted nonuniform grid, based on the idea of equidistribution principle. The error analysis for the numerical solution is carried out by

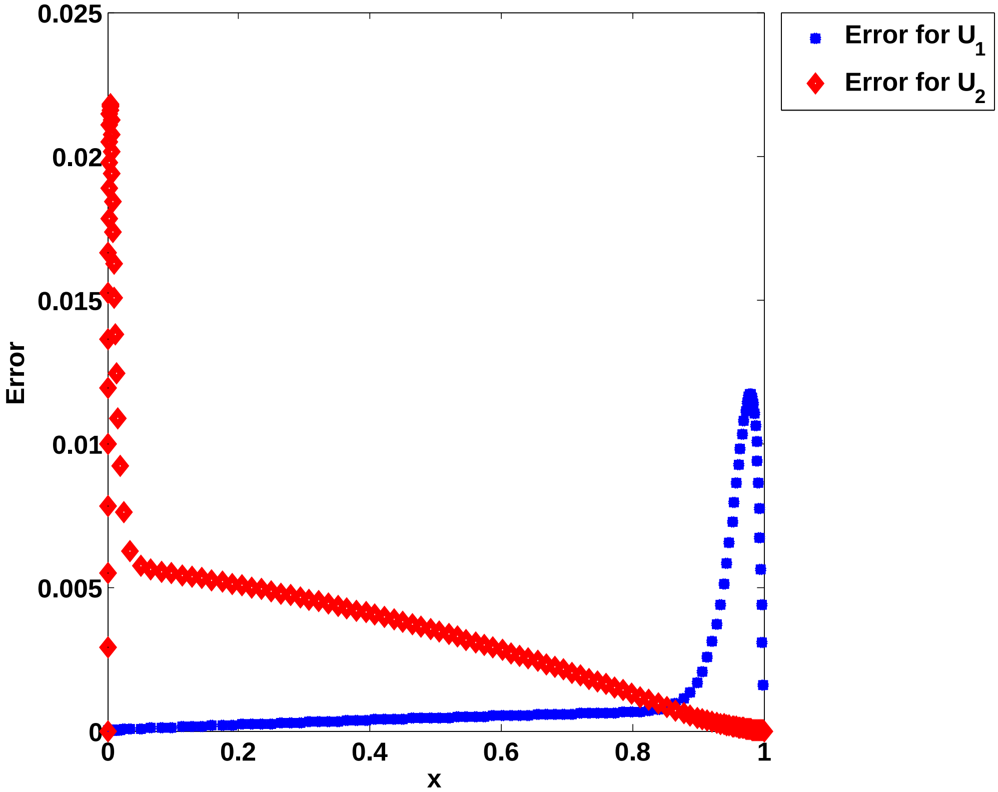

Figure 2: Error plot for U_1 and U_2 with $N = 128$ to the Example 5.2.

Table 5.4: Uniform errors and orders for u_2 for Example 5.2.

$(\varepsilon_1, \varepsilon_2) \in S$	Number of intervals N						
	64	128	256	512	1024	2048	4096
E_2^N	1.2823e-1	5.5770e-2	2.0224e-2	8.0535e-3	3.4903e-3	1.7726e-3	8.1647e-4
r_2^N	1.2012	1.4634	1.3284	1.2063	0.9775	1.1184	-

Table 5.5: Uniform errors and orders for u_1 for Example 5.3.

$(\varepsilon_1, \varepsilon_2) \in S$	Number of intervals N						
	64	128	256	512	1024	2048	4096
E_1^N	1.1940e-2	5.3763e-3	2.4913e-3	1.2613e-3	5.9573e-4	2.8808e-4	1.5506e-4
r_1^N	1.1511	1.1097	0.9820	1.0821	1.0482	0.8936	-

using the maximum norm. It is shown that the errors are first-order convergent, which are independent of the singular perturbation parameters. Numerical results, obtained for linear and semilinear system of BVPs, validate the efficiency of the proposed monitor function, which lead to first-order parameter uniform accuracy.

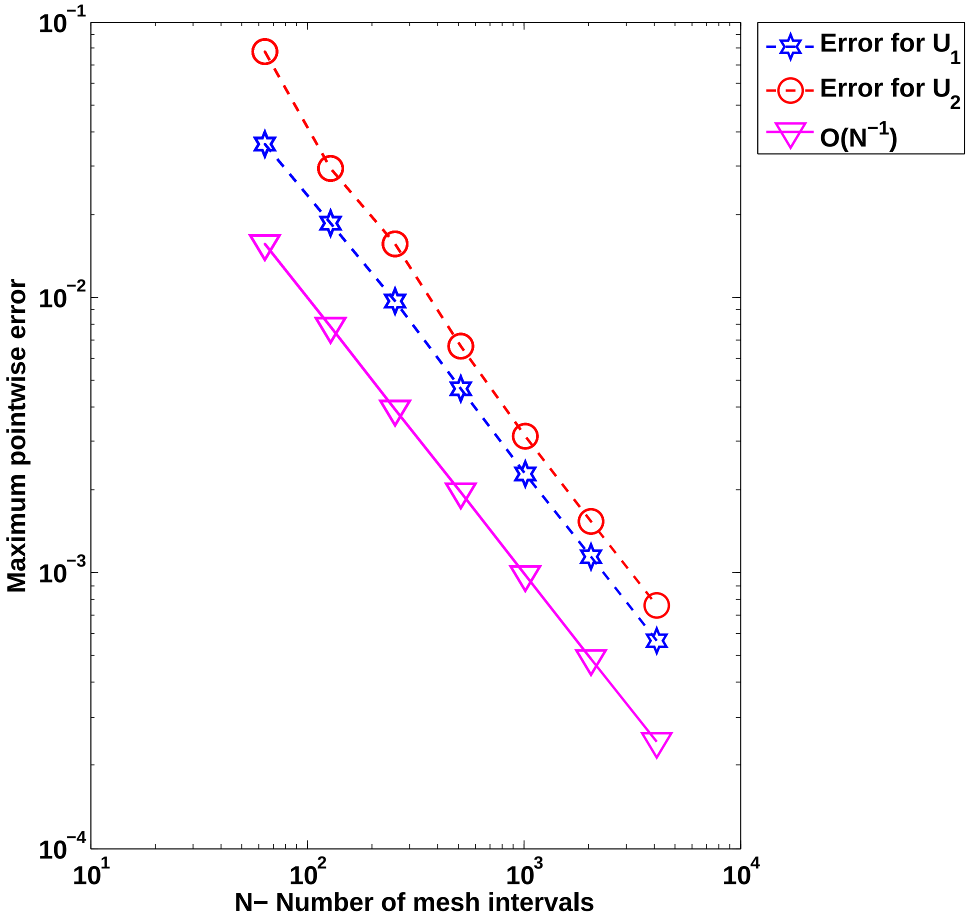

Figure 3: Error plot for U_1 and U_2 to the Example 5.2.

Table 5.6: Uniform errors and orders for u_2 for Example 5.3.

$(\varepsilon_1, \varepsilon_2) \in S$	Number of intervals N						
	64	128	256	512	1024	2048	4096
E_2^N	5.5380e-3	2.6561e-3	1.2129e-3	5.7023e-4	2.8811e-4	1.3645e-4	6.5712e-5
r_2^N	1.0601	1.1308	1.0889	0.9849	1.0782	1.0542	-

REFERENCES

[1] V. B. ANDREEV, The Green function and a priori estimates for solutions of monotone three-point singularly perturbed finite difference schemes, *Differ. Equ.*, **37** (2001), pp. 923-933.

[2] M. G. BECKETT, J. A. MACKENZIE, Convergence analysis of finite differences approximations on equidistribted grids to a singularly perturbed boundary value problem. *Appl. Numer. Math.*, **35** (2000), pp. 87-109.

[3] M. G. BECKETT, J. A. MACKENZIE, On a uniformly accurate finite difference approximation of a singularly perturbed reaction-diffusion problem using grid equidistribution, *J. Comput. Appl.*

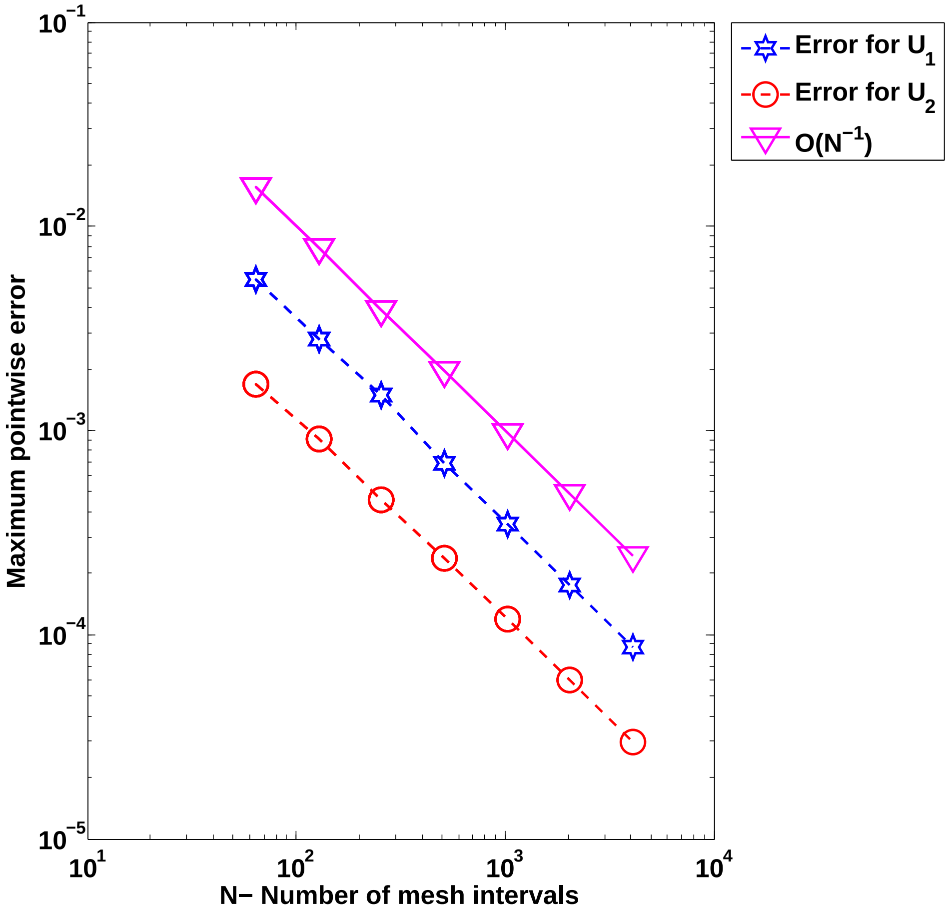

Figure 4: Error plot for U_1 and U_2 to the Example 5.2.

Math., **131** (2000), pp. 381-405.

[4] S. BELLEW, E. O'RIORDAN, A parameter robust numerical method for a system of two singularly perturbed convection-diffusion equations, *Appl. Numer. Math.*, **51** (2004), pp. 171-186.

[5] N. M. CHADHA, N. KOPTEVA, A robust grid equidistribution method for a one-dimensional singularly perturbed semilinear reaction-diffusion problem, *IMA J. Numer. Anal.*, (2011), pp. 188-211.

[6] K. W. CHANG, F. A. HOWES, Nonlinear Singular perturbation Phenomena: Theory and Applicatiosn, *Springer- Verlag, Berlin*, (1984).

[7] P. DAS, S. NATESAN, A uniformly convergent hybrid scheme for singularly perturbed system of reaction-diffusion Robin type boundary value problems. *J. Appl. Math. Comput.*, **41** (2013), pp. 441-471.

[8] E. P. DOOLAN, J. J. H. MILLER and W. H. A. SCHILDERS, Uniform Numerical Methods for Problems with Initial and Boundary Layers, *Boole Press, Dublin*, (1980).

[9] R. B. KELLOGG, A. TSAN, Analysis of some difference approximations for a singular perturbation problem without turning points. *Math. Comp.,* **32** (1978), pp. 1025-1039.

[10] T. LINSS, Analysis of an upwind finite-difference scheme for a system of coupled singularly perturbed convection-diffusion equations, *Computing,* **79** (2007), pp. 23-32.

[11] J. J. H. MILLER, E. O'RIORDAN and G. I. SHISHKIN, Fitted Numerical Methods for Singular Perturbation Problems, *World Scientific, Singapore,* (1996).

[12] H. G. ROOS, M. STYNES and L. TOBISKA, Robust Numerical Methods for Singularly Perturbed Differential Equations, *Springer Series of Computational Mathematics, 2nd Edition, Berlin,* (2008).

[13] C. ZHONGDI, Parameter Uniform finite dfference scheme for a system of coupled singularly perturbed convection-diffusion equations, *J. Syst. Sci. complex.,* **18** (2005), pp. 498-510.